Stem Cell Derived Extracellular Vesicles for Vascular Elastic Matrix Regenerative Repair

S Sajeesh[1], **Broekelman Thomas**[2], **P. Mecham Robert**[2], **Ramamurthi Anand**[1,3,*]

[1]Department of Biomedical Engineering, Cleveland Clinic, Cleveland, Ohio.

[2]Department of Cell Biology and Physiology, Washington University in St. Louis, St. Louis, Missouri.

[3]Department of Molecular Medicine, Cleveland Clinic Lerner College of Medicine of Case Western Reserve University, Cleveland, Ohio
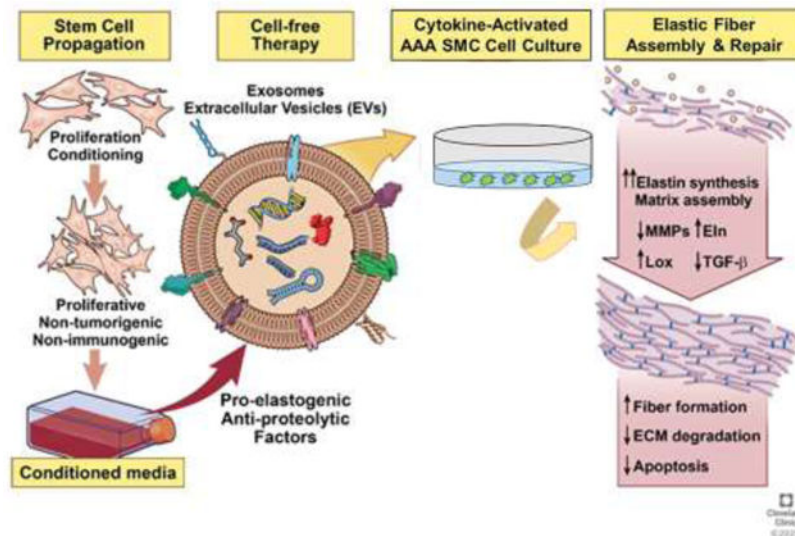
Abstract

Abdominal aortic aneurysms (AAA) are localized expansions of the abdominal aorta that develop due to chronic proteolytic disruption of the structural extracellular matrix (ECM) components (elastin and collagen) within the aorta wall. Major limitations in arresting or reversing AAAs lie in naturally poor and aberrant regeneration and repair of elastic matrix structures in the aorta wall. Bone marrow derived mesenchymal stem cells (BM-MSCs) have emerged as a promising regenerative tool and their therapeutic effects are also known to be effected through their paracrine secretions. Extracellular vesicles (EVs) present in these secretions have emerged as critical cellular component in facilitating many therapeutic benefits of MSCs. EV treatment is thus potentially appealing as a stem cell-inspired cell-free approach to avoid possible phenotypic plasticity of MSCs in vivo. In this study, we investigated the thus far unknown effects of BM-MSC derived EVs on vascular elastic matrix repair in the context of AAA treatment. EVs isolated from BM-MSC source were characterized and their pro-regenerative and their anti-proteolytic effects were evaluated on our established in vitro experimental conditions derived from AAA rat model. Our studies revealed the efficacy of BM-MSC derived EVs in attenuating the proteolytic activity and also in imparting elastic matrix regenerative benefits under aneurysmal environment. Interestingly, compared to cell culture conditioned media (CCM), EVs demonstrated superior regenerative and anti-proteolytic benefits in a proteolytic injury culture model of AAA. From these studies, it appears that EVs derived from BM-MSCs could be beneficial in undertaking a reparative effort in AAA induced degeneration of vascular tissue.

Graphical abstract

*Corresponding author: Anand Ramamurthi, Biomedical Engineering, 9500 Euclid Avenue, Cleveland, OH, 32901, Tel: (216) 444-4326, Fax: (216) 444-9198, ramamua@ccf.org.

1. Introduction

Multifactorial and complex in its nature, the pathogenesis of abdominal aortic aneurysms (AAAs) is largely attributed to chemokine-driven leukocyte infiltration in the aortic wall followed by local destruction of elastin and collagen in the medial layer by chronically overexpressed matrix metalloproteases (MMPs) [1–3]. Unlike other extracellular matrix (ECM) components of the vessel wall, elastic fibers which enable vessel stretch and recoil [4], are poorly restored upon injury due to poor elastogenicity of adult vascular cells [5, 6]. The regeneration and repair of elastic fibers thus represents a critical 'missing link' in natural tissue reparative responses to injury [7]. Lack of therapeutic approaches to stimulate elastic fiber neo-assembly in a proteolytic milieu represents a formidable challenge in tackling structural aberrations associated with these disorders [8, 9].

Mesenchymal stem cells (MSCs) represent a readily accessible autologous/allogeneic cell source exhibiting tissue reparative properties [10, 11]. MSCs have the potential for multi-lineage differentiation [12], and have been shown to possess limited risk of immunogenicity and rejection upon allogneic or xeno-transplantation [13]. In the current context, our prior studies have indicated that BM-MSCs with nascent smooth muscle cell (BM-SMCs) characteristics provided significant anti-proteolytic and pro-elastogenic impetus to aneurysmal SMCs, effected mainly through their paracrine secretions [14, 15]. Despite their beneficial matrix regenerative properties, the physical delivery of MSCs to the site of tissue repair has major clinical and translational challenges [16], the foremost being phenotypic plasticity of the stem cells in vivo [17]. A stem cell -inspired, but cell-free approach, for tissue repair that leverages the beneficial paracrine signaling mechanisms of stem cells can be a viable alternative with good potential for clinical translation [18].

In this context, extracellular nanovesicles (EVs) *aka* exosomes, lipid bilayer vesicles in the nanometer size range of 40–150 nm [19], have recently emerged as an important mediator in facilitating inter-cellular communications of a variety of different cell types [20]. As exosomes refer specifically to the EV fraction generated via endosomal pathway, and since current isolation techniques can generate vesicles of non-endosomal origin also, we henceforth refer to these vesicles as EVs [21]. EVs could thus represent the active component in the MSC secretome accountable for their reparative effects. Recent studies suggests that EVs transport the biologically active cargo (e.g., small RNAs, miRNAs and proteins) from MSCs to the sites of injury to stimulate and regulate regenerative effects in these tissues [22]. However, the effects of EVs on extracellular matrix (ECM) homeostasis and potential utility in elastic matrix regenerative repair are largely unknown. In this study, we thus investigate possible anti-proteolytic and pro-matrix regenerative effects of human BM-MSC derived EVs in a proteolytic injury culture model of rat aneurysmal SMCs. EVs effect on key signaling pathways that have been implicated in ECM homeostasis are also broadly assessed to provide some insight into the mechanistic basis of these EV effects.

2. Materials & Methods

2.1 Isolation of Human BM-MSC Derived EVs

BM-MSCs were commercially procured at passage 2 (Lonza; Walkersville, MD) and cultured in DMEM low glucose medium supplemented with 10% v/v MSC-qualified fetal bovine serum (FBS; Thermo Fisher Scientific; Waltham, MA) and 1% v/v penicillin-streptomycin (Pen-Strep; Thermo Fisher Scientific). For EV isolation, the BM-MSCs were seeded in tissue culture flasks (Area = 175 cm^2; Thermo Fisher Scientific), and proliferated until 60–70 % confluency. At this time, the culture medium was replaced with 10% v/v exosome depleted FBS (Exo-free FBS; Thermo Fisher Scientific)-supplemented medium, 48 h prior to isolation. The cell culture supernatant was collected thereafter and EVs were isolated by differential centrifugation method [23]. Briefly, culture medium was centrifuged at 300g for 10 min to remove dead cells and supernatant was further centrifuged at 2000g for 15 min and at 10,000g for 30 min. The supernatant was transferred into polycarbonate tubes and centrifuged at 100,000g for 70 min (Type 50.2 Ti rotor, Beckman Coulter, Fullerton, CA). The pellets were dispersed in phosphate-buffered saline (PBS) by gentle pipetting, and protein concentration was measured using bicinchonic acid (BCA) assay (Thermo Fisher Scientific).

Conditioned cell culture medium (CCM), which represents the totality of BM-MSC secretions, and CCM depleted of EVs (CCM-D) were used as control treatments in assessing matrix regenerative effects due to the EVs. CCM samples were prepared by centrifuging MSC culture media at 300g for 30 min and concentrated (10×) using Amicon® Ultra centrifugal filters (Millipore Sigma, St. Louis, MO; 10kDa MWCO). CCM-D samples were prepared by removing the EV component from the CCM sample by ultracentrifugation method, as mentioned above, and supernatant was concentrated (10×) using Amicon® Ultra centrifugal filters. Protein concentration in CCM and CCM-D samples was determined by BCA method.

2.2 Characterization of EVs

2.2.1 Nanoparticle Tracking Analysis (NTA) for EV Size and Concentration

—The size and concentrations of EVs in suspension, CCM and CCM-D samples were measured using ZetaView® (Particle Metrix GmbH, Germany). EV samples were assayed at 25 μg/mL protein concentration (1:800 dilution in PBS), while CCM and CCM-D samples were used at 1 mg/mL protein concentration (1:800 and 1:2 v/v dilution in PBS, respectively for CCM and CCM-D samples) for the NTA studies.

2.2.2 Transmission Electron Microscopy (TEM) to Confirm EV Ultrastructure

—TEM was used to confirm EV identity through visualization of their characteristic bilayered wall morphology and size. Briefly, the EVs were fixed in 4% w/v glutaraldehyde overnight and washed with PBS. The EVs were negatively stained with 2% w/v uranyl acetate and applied to a FCF 400-CU (400 Mesh) grid (Electron Microscopic Sciences; Hatfield, PA). The EVs were visualized on a FEI Tecnai Spirit T12 (Hillsboro, OR) transmission electron microscope.

2.2.3 Western Blot Analysis for Expression of EV Marker Proteins—The

isolated EV pellets were dispersed in RIPA buffer (Thermo Fisher Scientific) and assayed for total protein content using a BCA assay kit. Samples were loaded onto NuPAGE™ 4–12 % sodium dodecyl sulfate-polyacrylamide gel electrophoresis (SDS-PAGE) gel (Thermo Fisher Scientific), along with a SeeBlue™ pre-stained molecular weight ladder (Thermo Fisher Scientific). The gels were transferred onto nitrocellulose membranes (iBlot™ 2 Western Blotting System; Thermo Fisher Scientific), and blocked (Odyssey blocking buffer; LI-COR Biosciences, Lincoln, NE) for 1 h at room temperature. Primary antibody labeling was carried out on the membranes for 16 h at 4°C with corresponding monoclonal mouse antibodies (Thermo Fisher Scientific) at 1:1000 dilutions. Secondary antibody labeling was carried out for 1 h at room temperature using IR Dye 800CW goat anti-mouse (1:20,000 dilution) antibodies (LI-COR Biosciences). Protein bands were visualized on the immunolabeled membranes via fluorescent detection, using a LI-COR Odyssey laser-based scanning system.

2.2.4 Exosome Antibody Array—EVs were further characterized using Exo-Check

Arrays (System Biosciences, Palo Alto, CA) for positive expression of 8 known exosome marker proteins. Briefly, the array was exposed to 50 μg of EV samples and the assay was performed as per manufacturer's instructions. The membrane was developed with SuperSignal™ West Femto Maximum Sensitivity Substrate (Thermo Fisher Scientific) and analyzed using ChemiDoc.

2.3 Experimental Design to Assess the Effect of EV/CCM/CCM-D Treatment on EaRASMC Cultures

2.3.1 Isolation and Culture of SMCs from Elastase Injury-Induced Rat AAAs

(EaRASMCs)—All animal procedures were conducted with approval of the Institutional Animal Care and Use Committee (IACUC) at the Cleveland Clinic. The Clinic animal facility is AAALAC approved and has animal assurance (A3047-01, 12/31/21). Primary EaRASMCs were isolated from aneurysmal aorta explants obtained from adult male

Sprague-Dawley rats at 14 days post-AAA induction via elastase infusion [24], as we have previously published [25, 26]. The primary cells from three different animals were pooled and propagated for culture in DMEM/F12 medium containing 10% v/v fetal bovine serum (Thermo Fisher Scientific) and 1% v/v penicillin-streptomycin (Pen-Strep), with passaging performed at 70–80% confluence. Cells used in experiments were of passages 2–6.

2.3.2 Culture Study Design—The effects of EV/CCM/CCM-D treatment on gene and protein expression of key signaling proteins involved in ECM regulation homeostasis was investigated in a culture model of cytokine-injured EaRASMCs [27]. EaRASMCs were seeded in six-well plates (USA Scientific, Ocala, FL) at 30×10^4 cells per well and cultured for 14 days in DMEM F-12 medium containing 10% v/v FBS and 1% v/v Pen-Strep, with twice weekly medium changes. On day 14 post-seeding, the cultures were serum starved for 3 h in DMEM F-12 with 1% v/v Exo-free FBS and 1% v/v Pen-Strep. The cells were treated for 30 min with 10 ng/mL each of the cytokines, tumor necrosis factor- alpha (TNF-α; PeproTech, Rocky Hill, NJ) and interleukin-1 beta (IL-1β; R&D Systems, Minneapolis, MN) to exaggerate the AAA disease phenotype [28]. The medium containing cytokines was replaced with medium containing either EVs (25 μg/mL; total protein concentration) or with CCM or CCM-D (1 mg/mL; total protein concentration) for a period of 24 h in DMEM F-12 with 1% v/v Exo-free FBS. EaRASMC cultures treated only with cytokines, served as the treatment controls (TC) in these experiments.

For biochemical analysis of deposited elastic matrix and crosslinking of the matrix, the EaRASMCs were cultured for a total of 21 days [29]. The cells were subject to repeated cytokine injury and treated on day 7 and 14 post-seeding with either EVs (25 μg/mL; total protein concentration) or CCM/ CCM-D (1 mg/mL; total protein concentration) for a period of 24 h in DMEM F-12 with 1% v/v Exo-free FBS. Following each treatment event, the cultures were switched back to culture in regular culture medium composed of DMEM F-12 with 10% v/v FBS. The treated and control cell layers were harvested at day 21 post-seeding for biochemical analysis.

2.3.3 Assessment of Cellular Uptake of EVs in EaRAMSC cultures—For evaluating the cellular uptake of EVs, isolated vesicles were labeled with the CellVue® Red fluorescent labeling kit (Polysciences, Warrington, PA) according to the manufacturer's protocol. EaRASMCs grown in 35 mm Nunc™ glass bottom dishes (Thermo Fisher Scientific) were exposed to 50 μg/ml of labeled EVs in serum-free conditions for 2h. Surface-bound exosomes were removed by PBS washing and cells were fixed in 4% w/v paraformaldehyde. Cell layer was stained with CellMask™ Green Plasma Membrane Stain (Thermo Fisher Scientific) and then mounted with Vectashield® containing the nuclear stain 4′,6-diamidino-2-phenylindole, dihydrochloride (DAPI; Vector Laboratories, Burlingame, CA). Imaging was performed on a Leica SP8 confocal microscope (Leica Microsystems Inc., Buffalo Grove, IL).

2.4 Anti-Proteolytic Effects of Treatments in an EaRASMC Culture

2.4.1 RT-PCR Analysis for Gene Expression of MMPs and TIMPs—Total RNA was isolated from the 14 day cultures using an RNeasy mini kit (Qiagen, Valencia, CA) and

quantified using a Nanodrop™ (Thermo Fisher Scientific). An iScript cDNA synthesis kit (Bio-Rad, Hercules, CA) was used to synthesize cDNA using 500 ng of RNA from all the samples and reverse transcription was performed for a total of 40 min combining 5 min at 25°C, 30 min at 42°C, and 5min at 85°C according to the manufacturer's instructions. Real-time polymerase chain reaction (RT-PCR) was performed using an Applied Biosystems 7500 RealTime PCR system with Power SYBR Green Master Mix (Thermo Fisher Scientific), and relative gene expression was estimated using   Ct (Livak method) [30] with 18s as the endogenous normalizing gene. Primer sets were obtained from Real Time Primers (Elkins Park, PA) and details are provided in the Table 1.

2.4.2 Western Blot Analysis for MMP2,MMP9 and TIMP2 Protein Expression

—EaRASMC cultures were harvested in RIPA buffer containing Halt™ protease inhibitor (Thermo Fisher Scientific), and assayed for total protein content using BCA method. The samples were loaded onto either 10 % (MMPs) or 4–12 % (other proteins) SDS-PAGE gel under reducing conditions, along with a SeeBlue® pre-stained molecular weight ladder (Thermo Fisher Scientific). The gels were transferred onto nitrocellulose membranes and blocked in Odyssey blocking buffer for 1 h at room temperature. Membranes were labeled using rabbit polyclonal anti-rat antibodies against MMP2, MMP9 and TIMP2 (1:1000 dilutions, Abcam, Cambridge, MA), for 16 h at 4 °C, along with a mouse polyclonal antibody against β-actin (1:2000 dilution; R&D Systems, Inc., Minneapolis, M) as the loading control. Secondary antibody labeling was carried out for 1 h at room temperature using IR Dye 680LT goat-anti-rabbit (1:15,000 dilution) and IR Dye 800CW goat anti-mouse (1:20,000 dilution) antibodies (LI-COR Biosciences). Protein bands were visualized on the immunolabeled membranes using a LI-COR Odyssey scanning system and band intensity on membranes were quantified using Image Studio™ software, and normalized to that of their respective β-actin (loading control) bands, to enable comparison of different test cases within the same blot.

2.4.3 Gel Zymography for MMP2 Activity

—Enzyme activity of elastolytic MMP2 was assayed using gel zymography, as described in prior studies by our group [27]. Briefly, cell layers (harvested in RIPA buffer containing protease inhibitor) were loaded into each lane of a 10% zymogram gel (Thermo Fisher Scientific). The gels were run for 2 h at 125 V in Tris-glycine SDS running buffer. Gels were then washed in a zymogram denaturing buffer (Thermo Fisher Scientific) for 30 min to remove any traces of SDS, and incubated in zymogram developing buffer (Thermo Fisher Scientific) overnight to activate the MMPs. Finally, the gels were stained (30 min) with a SimplyBlue™ SafeStain solution (Thermo Fisher Scientific), and then distained in water, until clear bands were visibly apparent against the dark blue background of the gel. The intensities of the MMP2 bands in each case were measured using ImageJ software (National Institutes of Health, Bethesda, MD, USA).

2.5 Effects of Treatment on Elastic and Collagen Matrix Assembly in EaRASMC Cultures

2.5.1 RT-PCR Analysis for Gene Expression of Key Elastic Fiber Assembly

Proteins—The gene expression of key proteins implicated in ECM regulation and elastic fiber neo-assembly, upon EV/CCM/CCM-D treatment was assessed by RT-PCR analysis, conducted as described in section 2.4.1. The primer sets used to estimate gene expression

of elastin (ELN), collagen 1 (COL1), fibrillin-1 (FBN1), fibulin –4 (FBLN 4), fibulin-5 (FBLN5), lysyl oxidase (LOX) and lysyl oxidase like 1 (LOXL1) are stated in Table 1.

2.5.2   Western Blot Analysis for LOX and LOXL1 expression—LOX and LOXL1 protein expression were assessed by WB analysis performed on 14-day EaRASMC cultures that were cytokine-injured, then treated with EV/CCM/CCM-D. Primary antibody labelling was carried out using rabbit polyclonal anti-rat antibodies against LOX and LOXL1 (1:1000 dilutions, Abcam, Cambridge, MA), for 16 h at 4 °C. WB analysis was performed as described in section 2.4.2.

2.5.3   Immunofluorescence (IF) Detection of Elastic Matrix and LOX—Elastic matrix and LOX protein expression in control and treated EaRASMC cultures after treatment was visualized using IF. EaRASMCs were cultured for a total of 21 days in glass bottom chamber slides (Nunc™ Lab-Tek™ II Chamber Slide™ System, Thermo Fisher Scientific) with cytokine injury and treatments performed at day 7 and 14 post-seeding. At the end point, the cell layers were washed with PBS and fixed in ice-cold methanol (20 min). Cells were blocked in PBS containing 5% v/v goat serum (Thermo Fisher Scientific; 20 min) and immunolabeled with rabbit anti-rat polyclonal antibody against LOX protein and Elastin (1:100 v/v dilution, Abcam; 16 h at 4 °C). The protein was visualized by labeling with an AlexaFluor 546 goat anti-rabbit (1:1000 v/v dilution, Thermo Fisher Scientific) secondary antibody (1 h, 25 °C, dark). The cell layers were mounted with Vectashield® containing DAPI. EaRASMC layers designated as IF controls received only the secondary antibody and imaging was performed on a Leica SP8 confocal microscope.

2.5.4   Fastin Assay for Elastic Matrix—Matrix elastin content in the EaRAMSC cell layers was determined by Fastin assay [31]. Briefly, the 21 day culture cell layers (control and treated) harvested in Pi buffer were digested in 1.5 M oxalic acid (95 °C, 90 min), and pelleted by centrifugation at 14,000 g. The supernatant containing soluble α-elastin was separated out and the remaining pellet was further digested in 0.25M oxalic acid (100°C, 60 min). The digestate was centrifuged and the supernatant was pooled with the first α-elastin supernatant fraction. The elastin content in the pooled supernatant was measured using a Fastin™ Elastin assay kit (Accurate Chemical and Scientific Corp, Westbury, NY), as per manufacturer's instructions. The measured elastin content in the samples was normalized to their corresponding cell content determined using Fluorometric DNA assay [32], assuming per cell DNA content to be 6 pg.

2.5.5   Estimation of Desmosine Crosslink Content and Collagen Matrix Amounts—Cell layers obtained from 21 day cultures were harvested in PBS and pelleted by centrifugation (500 g, 5 min). Samples were then hydrolyzed with 6N HCl (105 °C, 48 h), evaporated to dryness and reconstituted in water. Desmosine levels in the samples were determined using a competitive ELISA assay [33] and normalized to the protein content in each sample aliquot, which was measured using Ninhydrin assay. Hydroxyproline assays were used to estimate matrix collagen content [33]. Samples oxidized with chloramine-T (Sigma-Aldrich) were combined with p-dimethylaminobenzaldehyde (Sigma-Aldrich) and absorbance was measured at a wavelength of 550 nm. Using hydroxyproline standard curve,

collagen amounts in the samples were calculated based on 13.5% w/w hydroxyproline content of collagen.

2.5.6 TEM to Assess Elastic Matrix Ultrastructure

The ultrastructure of the deposited elastic matrix was visualized using TEM, as we have previously described [27, 29]. Following 21 days of culture on Permanox chamber slides (Thermo Fisher Scientific), with cytokine injury and treatment regimens performed weekly as described in section 2.3.2, the cell layers were rinsed with PBS (37 °C), fixed initially in 2.5w/v glutaraldehyde in 0.1M sodium cacodylate buffer (37 °C, 5 min) and then overnight at 4 °C. The cell layers were then dehydrated in a graded ethanol series (50–100% v/v), embedded in Epon 812 resin and sectioned placed on copper grids, stained with uranyl acetate and lead citrate. Elastin deposits and elastic fibers were visualized on a FEI Tecnai G2 Spirit BioTWIN (Hillsboro, OR) TEM.

2.6 Effects of Treatment on ECM Signaling Pathways

2.6.1 Western Blot and RT-PCR Analysis

Expression of key signaling proteins implicated in ECM regulation and homeostasis were evaluated on EaRASMC by WB analysis. Primary antibody labelling was carried out using rabbit polyclonal anti-rat antibodies against TGF-β1 (1:500 dilutions, Abcam); JNK1/2/3 and ERK1/2 (1:1000 dilution, Abcam); and p38 MAPK (1:1000, Cell signaling Technology Danvers, MA). Experiments and analysis were performed in an exact manner as described in section 2.4.2. For determining the levels of phosphorylated pERK1/2 and pJNK, EaRAMSC cultures were first exposed to EV/CCM/CCM-D treatment for 24h in DMEM F-12 media supplemented with 1% v/v Exo-free FBS. After removing the culture medium, cells were treated with 1% v/v Exo-free FBS-supplemented medium containing 10 ng/mL cytokines (IL-1β and TNF-α) for 30 min. After removing medium containing cytokines, cells were further incubated in 1% v/v Exo-free FBS-supplemented DMEM F-12 medium and phosphorylated protein (pERK 1/2 and p-JNK) levels were determined at 30 min and 3h post-cytokine treatment with western blot, using their corresponding polyclonal anti-rat antibodies (p-ERK1/2 1:1000 dilution, Cell signaling Technology; p-JNK 1:1000 dilution R&D Systems). RT-PCR analysis was performed to calculate the relative gene expression of TGF-β1 in an exact manner as described in section 2.4.1, using specific primer set (Table 1).

2.6.2 ELISA for TGF-β1 Expression

Mature TGF-β1 secreted into the cell culture medium, after EV/CCM/CCM-D treatment for 24 h were collected from a 14 day EaRASMC culture model. TGF-β1 level were quantified using rat TGF-β1 ELISA kit (Abcam) as per the manufacturer's instructions.

2.6.3 Antibody Array

RayBio® L-Series Rat Antibody Array 90 (RayBiotech Life, Peachtree Corners, GA) was used to assess a broader view on cytokine expression, following treatment with EVs or CCM in a 14 day culture model. Cell lysate from EaRASMC treated with either EVs (25μg/mL) or CCM treatment (1 mg/mL) was subjected to L-90 antibody array experiments, alongside EaRASMC (TC), following manufacture's standard protocol. The analysis was performed with the manufacturer's recommended protocol, and the signals

of Cy3 were imaged by Axon GenePix 4000 laser scanner (MDS analytical technologies, Sunnyvale, CA).

2.7 Statistical Analysis

A non-parametric test (Mann-Whitney test) was used to determine differences between the treatment groups, as indicated in the figure legends. Statistical analyses were run using Prism 8 (GraphPad Software Inc.). Data are presented as means ± SE. Differences were considered statistically significant when the p value was   0.05. In the results below, p values are indicated only for statistically significant outcomes.

3.   Results

3.1   Isolation, Characterization and Cellular Uptake of EVs

NTA showed that the average diameter for isolated EVs was 99±1 nm (Fig 1A) and their particle concentration was ~4.5×10^8 particles/mL at 25 μg/mL (total protein content). Particle concentration in CCM samples were adjusted to be in the same range as that of EV isolates for direct comparison of the effects on cells. As per NTA studies, CCM samples containing a total protein content of 1 mg/mL contained ~6.5×10^8 particles/mL, with an average diameter of 85±1 nm. Due to the similarity in their EV content, further studies were performed using a suspension of EVs at 25 μg/mL and CCM at 1 mg/mL based on total protein content. Samples designated as CCM-D, containing an identical total protein concentration of 1 mg/mL contained far fewer particles (~3×10^7 particles/mL) when analyzed by NTA, confirming the depletion of EVs from the CCM sample. TEM imaging (Fig 1B) showed the negative stained particles to exhibit the classical bi-layered membrane morphology of EVs, and to be in the anticipated size range (80–140 nm) in agreement with the NTA measurements.

WB blot analysis showed the isolated particles to express EV-specific marker proteins CD63, CD-9 and TSG101 (Fig 1C). In addition, the EVs showed positive expression of the mesenchymal cell specific marker vimentin. The exosome antibody array performed on the EV samples further confirmed the expression of common protein markers of EVs (FLOT1, ICAM, ALIX, CD81, CD63, ANXA5 and TSG 101) (Fig 1D, Table S1). GM130 cis-Golgi marker and EpCAM were not expressed by the EVs. Further, cellular uptake investigations clearly demonstrated that fluorescently labeled EVs were effectively internalized by the EaRASMCs (Fig S1).

3.2   Effect of Treatment on Expression of Elastolytic Enzymes

RT-PCR analysis (Fig 2A) demonstrated reduced MMP2 gene expression in EV and CCM treated cultures versus TC cultures. MMP2 gene expression was 0.6 ± 0.1 fold (p = 0.04), 0.3 ± 0.1 fold (p = 0.004) and 0.7 ± 0.1 fold respectively in EV, CCM, and CCM-D treated cultures relative to that in TC cultures. EV treatment resulted in 2 ± 0.3 fold (p = 0.02) and 3 ± 0.8 fold change in gene expression of TIMP1 and TIMP2 respectively, relative to that in TC cultures. No significant changes in the gene expression of TIMP1 and TIMP2 were noted in cultures treated with either CCM or CCM-D against the TC cultures, while MMP 9 gene expression was not detected in any of the cultures.

MMP2 protein levels analyzed by WB are shown in Fig 2B. In TC cultures, only the active MMP2 band (62–66 kDa), not the MMP2 zymogen band (72 kDa), was detected. When treated with EVs, expression of the MMP2 zymogen band was significantly increased (6 ± 0.4 fold vs TC, p = 0.002), while expression of active MMP2 band was reduced (0.1 ± 0.05 fold vs TC, p = 0.002). However, total MMP2 level (zymogen MMP2 + active MMP2) was unaffected with EV treatment (0.8 ± 0.1 fold vs TC). EaRASMC that received CCM showed significantly higher expression of MMP2 zymogen (12 ± 2 fold vs TC, p = 0.002) and active MMP2 (3 ± 0.4 fold vs TC, p = 0.002), which led to significant enhancement in total MMP2 expression (4 ± 0.4 fold vs TC, p = 0.002). Treatment with CCM-D elicited maximal increase in relative expression of MMP2 in our study, with MMP2 zymogen band intensity increased by 22 ± 2 fold vs TC (p = 0.002) and active MMP2 band by 5 ± 0.5 fold vs TC (p = 0.002), contributing to 7 ± 0.6 fold increase in expression of total MMP2 vs TC (p = 0.002).

WB analysis for TIMP2 protein expression is shown in Fig 2C. Cultures which received EV treatment demonstrated increase in TIMP2 expression (3 ± 0.3 fold vs TC, p = 0.004). TIMP2 expression was changed 2 ± 0.2 fold vs TC (p = 0.03) and 2 ± 0.3 fold vs TC, with CCM and CCM-D treatments respectively. The ratio of active MMP2/TIMP2 obtained from WB analysis is shown in Fig 2D. MMP2/TIMP2 ratio for TC cell layers was 2 ± 0.4, and the ratio was dropped to 0.06 ± 0.03 (p = 0.002 vs TC) for EV treated cultures. CCM treatment had limited impact in MMP2/TIMP2 ratio (2 ± 0.4), while CCM-D treatment caused a significant increase in the ratio (5 ± 1, p = 0.002 vs TC). Compared to MMP2 protein, MMP-9 protein expression was consistently low in both TC and treated cultures. EV/CCM/CCM-D treatment were seen to further reduce MMP 9 levels in EaRASMC cultures compared to TC cultures (Fig S2), and EV treatment appeared to be most effective in this regard. TIMP-1 proteins were not detected in any of the cultures. Gel zymography results (Fig. 2E) suggest that MMP2 enzyme activity in EV treated cultures was decreased to 0.4 ± 0.04 fold vs TC (p = 0.002). MMP2 enzyme activity was largely unaffected with CCM treatment (0.8 ± 0.2 fold vs TC), however, CCM-D treatment resulted in increased MMP2 activity (2 ± 0.2 fold vs TC, p = 0.02). MMP 9 activity was not detected in zymogram analysis of our samples.

3.3 Effect of EV/CCM/CCM-D Treatment on Elastic Matrix Assembly

Results from RT-PCR analysis used to evaluate the treatment-specific changes in the relative expression of selected genes involved elastic matrix homeostasis (ELN, FBN1, FBLN4, FBLN5, LOX and LOXL1) and COL1 are presented in Fig 3A. Expression of ELN, FBN1, FBLN4 and FBLN 5 were 2 ± 0.2 fold vs TC (p = 0.008), 4 ± 1 fold vs TC, 5 ± 2 fold vs TC, and 3 ± 0.6 fold vs TC (p = 0.008) respectively in EV-treated cultures, and 1 ± 0.2 fold, 3 ± 1 fold, 4 ± 2 fold, and 2 ± 1 fold vs TC (p = 0.03) respectively in CCM-treated cultures. Expression of these same genes were 1 ± 0.2 fold vs TC, 2 ± 0.6 fold vs TC, 3 ± 1 fold vs TC, 2 ± 0.3 fold vs TC (p = 0.04) in CCM-D-treated cultures. Relative gene expression of LOX was 3 ± 0.5 fold vs TC in RT-PCR analysis with EV treatment, while the expression of LOX L1 was 1 ± 0.2 fold vs TC. CCM and CCM-D treatment had no effect on gene expression of LOX (0.6 ± 0.3 fold vs TC for CCM and 0.8 ± 0.3 fold vs TC for CCM-D)

and LOXL1 (1 ± 0.2 fold vs TC for CCM and 1 ± 0.2 fold vs TC for CCM-D). COL1 gene expression was not impacted by EV/CCM/CCM-D treatment at the tested doses.

Results of WB analysis performed to evaluate LOX protein level expression are shown in Fig 3B. LOX protein expression was changed 3 ± 1 fold vs TC upon EV treatment, while LOX L1 level was 0.8 ± 0.3 fold vs TC. LOX and LOX L1 protein expression were not impacted by either CCM treatment (0.7 ± 0.1 fold vs TC and 0.9 ± 0.3 fold vs TC, for LOX and LOX L1 respectively) or CCM-D treatment (0.9 ± 0.5 fold vs TC and 1 ± 0.3 fold vs TC, for LOX and LOX L1 respectively).

Detection of LOX protein and elastin expression (Red) in our EaRASMC culture model at 21 days is shown in Fig 3C. Consistent with WB studies, cells treated with EVs stimulated the maximal relative increase in expression of LOX protein and deposition of elastic matrix. CCM treatment also had positive influence in improving LOX protein and elastin expression relative to TC, however to a lesser extent compared to EV-treated cultures. CCM-D treatment did not increase expression of LOX protein and elastic matrix deposition in the EaRASMC cultures.

The results of the Fastin assay (Fig 4A) showed that the total matrix elastin deposition in TC cultures (0.2 ± 0.01 μg/cell) was increased upon EV treatment (0.3 ± 0.02 μg/cell, p = 0.002 vs TC) and CCM treatment (0.2 ± 0.02 μg/cell, p = 0.008 vs TC), but not with CCM-D treatment (0.2 ± 0.01 μg/cell). Desmosine crosslink content for EV treated EaRAMSC cultures were 110 ± 13 pmole des/mg, while desmosine content in TC cultures were 88 ± 7 pmole des/mg (Fig 4B). Desmosine crosslink content for CCM and CCM-D treatment EaRAMSC cultures were 76 ±8 pmole des/mg and 86 ± 8.8 pmole des/mg, respectively. Results of the hydroxyproline assay (Fig. 4C) indicated no significant differences in the collagen synthesis between the different culture groups.

TEM images (Fig 5) showed presence of a homogenously dense matrix composed of maturing elastic fibers in the EV treated samples versus TC. CCM treatment increased elastic matrix deposition in EaRASMC cultures, however noticeably less dense elastic matrix deposition was observed in the CCM treated cultures, compared to EV treated cultures. In contrast, elastic fiber deposition was extremely poor in CCM-D treated cultures even relative to TC.

3.4 Effect of EV/CCM/CCM-D Treatment on Key ECM Regulating Pathways

ERK1/2 expression in EV-treated cultures was 0.6 ± 0.3 fold vs TC cultures (Fig 6A). ERK 1/2 expression in CCM-treated cultures was 2 ± 1 fold vs TC and 2 ± 1 fold in CCM-treated cultures vs TC cultures. Other key signaling proteins involved in the MAPK activation (JNK1/2 and p-38 MAPK) was not influenced with any of the treatments, under the tested experimental conditions (Fig 6B and 6C). Expression of pERK was increased with EV and CCM pretreatments, compared to TC, 30 min post-cytokine treatment. However pERK levels dropped with EV/CCM/CCM-D treated samples at 3h post-cytokine treatment (Fig S3), although the differences in outcomes between the treatments and TC were mostly not significant. On the other hand, pJNK levels were unaffected by treatment with EV/CCM/ CCM-D, when analyzed 30 min post-cytokine treatment (Fig S4) and pJNK was undetected

after 3h of incubation. The protein level expression of latent TGF-β1 was reduced by 0.5 ± 0.1 fold vs TC (p = 0.04), upon EV treatment (Fig 6D). However latent TGF-β1 expression was unaffected with CCM (0.9 ± 0.1 fold vs TC) or CCM-D treatments (0.6 ± 0.1 fold vs TC). Expression of Smad 2/3 was also unaffected with EV/CCM/CCM-D treatments (Fig S5). Relative expression of TGF-β1 gene was not influenced with EV/CCM/CCM-D treatments in our study (Fig 6E). Level of matured TGF-β1 quantified by ELISA method is presented in Fig 6F. Mature TGF-β1 level in TC culture was 65 ± 16 pg/mL, and EV treatment caused decrease in level of secreted TGF-β1 (11 ± 2 pg/mL, p = 0.04 vs TC). CCM and CCM-D treated EaRAMSCs had limited influence in the secretion of TGF-β1 in our study (65 ± 18 pg/mL and 27 ± 9 pg/mL for CCM and CCM-D treated cells respectively).

Semi-quantitative analysis from antibody array experiments revealed that EV treatment reduced the expression of pro-apoptotic and inflammtory cytokines, compared to the TC cells (Fig 7). EV treatment had promising outcomes in decreasing expression of cytokines involved in stimulating or facilitating apoptosis (e.g., TRAIL,TNFRSF6, FSL1), and also in increasing expression of cytokines involved in stimulating tissue repair and angiogenesis (e.g., FGF-BP, ICAM-1). On the other hand, CCM treatment induced higher expression of several pro-apoptotic and inflammatory cytokines, including TRAIL, TNFRSF6 etc.

4. Discussion

We investigated the role and utility of adult stem cell-generated EVs for augmenting in situ regenerative repair of elastic matrix, in the context of treating AAAs. Adult SMCs, more so aneurysmal SMCs, poorly regenerate elastic matrix and these cells cannot overcome accelerated elastolysis in a proteolytic mileu, to reinstate healthy elastic matrix structures [34]. Our previous investigations exploring the utility of adult BM-MSCs for vascular elastic matrix regenerative repair have established the critical role played by the CCM in stimulating production of elastin precursor and matrix deposition, in addition to their ability to attenuate proteolysis in aneurysmal SMC cultures [14, 15]. As the CCM contains several paracrine signaling factors, including metabolites, growth factors, and extracellular matrix proteins secreted into the medium by the cultured cells [18, 19], the active component(s) in the CCM responsible for these regenerative benefits is currently unknown. Several studies have implicated prominent role of EVs in mediating functional benefits associated with paracrine signaling and immunomodulatory functions of stem cells [20,22]. Our study focus was to understand if EVs are necessary and sufficient mediators of pro-elastogenic and anti-proteolytic effects exhibited by CCM, derived from a stem cell source. Specifically, the impact of EVs on elastogenesis and chronic proteolysis associated with aortic aneurysms has not been evaluated, and forms the basis of current investigation. As an added advantage, delivery of EVs would circumvent the uncertainties associated with physical delivery of cells, such as in vivo phenotypic plasticity, and poor cell engraftment at the injury site [12].

We used a sequential centrifugation method, which separates particles according to their buoyant density by centrifugation, to isolate EVs from BM-MSCs. EVs were isolated by high speed centrifugation (100,000 g) after removing the cells and larger particles at low speed centrifugation steps [22]. Since the study involves the comparison of EVs and CCM,

we normalized the particle content in the isolated EV samples and CCM samples, via NTA analysis. This allowed us to directly compare the regenerative effects due to EVs and the CCM samples. Compared to isolated EVs, the EV component present in the CCM samples showed smaller average particle size in the NTA studies. This can be attributed mainly due to the interference from non-EV particulate components present in the CCM samples, which likley contributed to a smaller average particle size. Significantly, EV-depleted CCM samples containing a similar total protein concentration as in the CCM were also assessed to ascertain the contribution of non-EV components of the CCM to the studied outcomes. Presence of specific marker proteins (CD63, CD-9 and TSG101), the bilayered wall structure and average size of isolated particles confirmed their identity as EVs. Positive expression of mesenchymal specific marker, vimentin, established the stem cell lineage of the isolated EVs [35]. The absence of expression of the Golgi subfamily A member 2 (GM130), a component of the cis-Golgi stack, showed the lack of cellular contamination in our EV preparations, while absence of EpCAM marker expression indicated non-cancerous origin for the isolated EVs. Our results presented in Fig S1 showed that the EVs internalize within EaRASMCs. Literature suggests that the functional outcomes elicited by EVs in target cells are a function of their mechanism of internalization, with engagement of the endosomal-lysosomal pathway through phagocytosis and endocytosis leading to EV degradation and not cellular responses in the manner elicited soluble, juxtacrine, and fusion mechanisms [36]. Although this is not a focus of the present study, the functional outcomes elicited by the EVs in our EaRASMCs suggest their uptake by the latter, non-endosomal mechanisms.

De novo assembly of elastic fibers is a complex, multi-step process mediated by several proteins that act in a coordinated manner. Our culture model of cytokine injured rat aortic SMCs is an ideal platform to investigate this, as it allows us to isolate the effects of simulated proteolytic milieu on steps involved in elastic fiber assembly, which cannot be studied in vivo as the latter only provides information on net changes to matrix homeostasis. In the future our culture model can be extended further to test effects of other parameters relevant to the AAA milieu such as matrix debridement by inflammatory cells, signaling by thrombus-derived cellular factors, etc. on elastin degradation, SMC phenotype, and new elastic matrix assembly. Our studies have also confirmed that cytokine injury model of cultured AAA SMCs cultures maintained their viability and morphology after 21 days in culture. Cytokine dose and treatment duration (10 ng/mL for 30 min) used in our studies was optimized to have minimal impact on the viability and phenotype of aneurysmal SMCs [26, 27].

Our results provide strong evidence that the EVs attenuate proteolytic activity in the EaRASMC culture model. A critical finding is that EV treatment reduces the expression of elastolytic MMP2, which is centric to AAA etiology [3], particularly in small, growing AAAs [37]. EV treatment also caused an increase in the expression of natural tissue inhibitor of MMP2 (TIMP2) and significant downfall in the ratio of MMP2/TIMP2, suggesting a robust anti-proteolytic milieu generated with EV treatment. Further observation that CCM and CCM-D treatment caused an increase in the overall expression of MMP2 suggest a critical roleplayed by EVs in governing proteolytic activity. CCM, which represents the totality of the cell secretions, contains several contributing factors that

may induce a net increase in proteolytic activity. This was quite evident with antibody array experiments, as the CCM treatment on EaRASMC culture led to the upregulation of several pro-inflammatory and pro-apoptotic cytokines. Presence of these contributing factors might dominate and this could marginalize the anti-proteolytic effects imparted by EV component in CCM. However, when the majority EV component was depleted from CCM, the expression of MMP2 was further enhanced. This observation possibly suggest that EVs play a critical role in attenuating proteolytic activity, since their absence exacerbates the proteolytic environment. Although MMP9 also plays a central role in AAA pathophysiology, their constitutive expression by SMCs in cultures is generally very low [38]. In our study, this is expected since the EaRASMCs are isolated from small aneurysmal expansions wherein MMP2 is primarily overexpressed [37] unlike larger, rupture prone AAAs wherein MMP9 overexpression is the primary determinant of ECM breakdown [39]. In AAAs in vivo, MMP9 is primarily expressed by macrophages, and by SMCs in response to macrophage-generated cytokines. Accordingly, in this study, we have sought to enhance MMP9 expression by cytokine-stimulation of our EaRASMCs, although our focus remains on attenuating MMP2 attenuation expression in the context of future treatment of small AAAs. Nevertheless, our results (Fig S2) do indicate an overall trend in reducing MMP9 expression in EaRAMSC cultures, when treated with EVs.

Our observations as to the increase in LOX expression upon EV treatment implies the benefits in terms of increasing deposition of a crosslink stabilized and fibrous elastic matrix in aneurysmal SMCs. Consistent with increased expression in LOX protein, we also measured higher amounts of desmosine crosslinks within the cell layers treated with EVs, although due to the small sample size, and likely variability imposed by testing pooled cultures of EaRASMCs sourced from different animals, the differences in desmosine amounts between the EV-treated and TC cultures was deemed to be just below the threshold for statistical significance. Regardless, the results suggest benefits of EV treatment to improved elastic matrix crosslinking and resistance to proteolytic disruption that might be realized with further testing with a greater number of replicate cultures to ensure statistical significance.

Total elastin deposition, as quantified by Fastin assay, also confirmed the ability of EVs to enhance deposition of elastic matrix in EaRASMC cultures, while collagen level in the EaRASMC cultures was largely unaffected with EV treatment. This might have a positive impact in treating AAAs, as elastin breakdown is usually accompanied with collagen build-up within the aortic wall, and this might adversely affect the wall hemostasis leading to a continued deviation of collagen to elastin ratios from healthy levels and increased wall stiffness. Outcomes of IF and TEM imaging were consistent with the biochemical assay outcomes in demonstrating the enhanced assembly of elastic fibers in the process of maturation in the EV treated EaRASMC cell layers. This could be attributed to increased elastin synthesis by EaRASMCs upon EV treatment, besides across the board increases in gene expression of key proteins critical to elastic fiber assembly such as fibrillin-1 (glycoprotein pre-scaffold on which elastin is deposited and crosslinked), and fibulin 4 and fibulin 5, which act in concert to chaperone tropoelastin and LOX to be directed onto microfibrils for fiber assembly [40]. Treatment with CCM also demonstrated a positive impact in enhancing the elastin deposition in EaRASMC cell layers, even though CCM

treatment had minimal impact in the expression of LOX or desmosine crosslinks. Presence of several tropic factors (growth factors and other stimulating factors) could be responsible for this pro-elastogenic effect imparted by CCM, which needs to be investigated further. However, no apparent difference in density and formation of elastic matrix were observed for cell layers exposed to CCM-D, compared to TC cultures. This observation clearly suggests that EVs are necessary component in BM-MSC secretions important to their elastic matrix regenerative and anti-proteolytic properties.

The precise cellular mechanisms by which EVs exert their functional benefits to elastic matrix assembly remain unclear and needs to be elucidated for developing an effective treatment approach. MAPK signaling pathways are critical regulators of MMPs and fundamental MAPK signaling pathways includes the ERK-1/2, JNK, and p38 pathways, mediate key intracellular signaling and communications [41]. Extracellular signal-related kinase (ERK) is an important modulator of MMPs and major contributor for AAA pathogenesis [42], our studies demonstrated an overall trend in the reduction of ERK1/2 expression, though the values failed just below the threshold for statistical significance. Consistent with anti-proteolytic investigations, treatment with CCM and CCM-D also caused an increasing trend in ERK1/2 expression in EaRASMC culture. In this study the other major pathways (JNK and p38) were not influenced upon treatment with EVs, after a period of 24 h. Levels of phosphorylated proteins (pERK and pJNK) were analyzed post-cytokine treatment, as our original protocol involving treatment of EaRAMSCs with inflammatory cytokines (IL-1β+TNF-α) followed by 24h treatment with EV/CCM/CCM-D was not conducive in detecting the above phosphorylated signaling proteins, possibly due to their transient expression profile. Consistent with ERK1/2 results, EV/CCM/CCM-D treatments were effective in attenuating the expression of pERK at 3h post-cytokine treatment, though a transient increase in pERK expression was observed with EV and CCM treatments at the 30 min time point. Our results suggest that both JNK and their phosphorylated version (pJNK) are minimally impacted with EV treatment. However, we will clarify these findings through a focused and rigorous future investigation of the effects of the stem cell secretions on signaling protein expression as a function of time.

Another key aspect was to study the effect of EVs on TGF-β signaling. TGF- β have a paradoxical role in AAA pathogenesis and investigations have supported both their pathogenic and protective roles [43]. TGF- β is known to stabilize aneurysmal expansion, however, at an advancing age, TGF-β has been also associated with arterial stiffness which is linked to loss of elasticity and increased stiffness within the arterial wall [44]. Our results suggest that the EV treatment reduced overall TGF-β expression, both in its latent form and mature form, however the levels of Smad2/3 was unaffected with EV treatment. It is unclear how EV treatment is involved in the regulation of TGF- β signaling and this needs to be further investigated. One possible explanation could be the presence of EV surface enzymes, which retains their activity and might degrade their natural substrates present within extracellular spaces. EVs harbor both active and latent TGF β on their surfaces, and once endocytosed, they influenced the recipient cell migratory phenotype [45]. Presence of exosomal TGF- β might reduce the overall expression of TGF- β exhibited by EaRASMC cell layers and this might also influence the expressions of MMPs. TGF-β and MMPs function in a bidirectional regulatory loop, as TGF-β needs to be activated proteolytically by

MMPs and TGF-β modulates ECM balance by regulating the expression of MMPs and their tissue inhibitors TIMPs [46]. A reasonable explanation at this stage for reduced proteolytic activity could be explained based on reduced TGF-β expression caused by EV intervention, however any conclusive statement at this stage will be largely pre-mature.

The emphasis in this study was to seek initial evidence of the pro-elastogenic and anti-proteolytic effects of BM-MSC-derived EVs. Our study of rat aneurysmal SMCs and not human SMCs was motivated by our requirement to perform a subsequent controlled and systematic in vivo investigation of EV biodistribution and therapeutic benefits in rat elastase injury model, since clinical study involving AAA patients is not feasible at this stage. However, this is not a significant limitation to future translation of this work since rat AAA SMC culture model is a good surrogate for study of human AAA SMCs. We have shown in prior published studies that rat aneurysmal SMCs closely resemble human AAA SMCs in their phenotype, poor elastogenicity, and positive response to elastogenic stimulation using exogenous factors [26,47]. This is because the rat elastase injury AAA model closely replicates to the mode of vascular wall injury in human AAAs (from the lumen outwards and based on elastic matrix breakdown), human AAA pathophysiology, and similarity in that percentage size change of the aorta depends on wall remodeling events [25, 26].

A limitation of this study is that the paracrine secretions (CCM, EVs, CCM-D) were collected from a single human BM-MSC cell line, and thus the study does not factor in the variability in content, and phenotypic profile of EVs drawn from multiple individuals. This will be the basis for our planned follow up study, wherein we will also perform proteome profiling of various batches of EVs and further assess their matrix regenerative benefits as a function of dose, as aspect that was not studied in the current exploratory study.

5. Conclusions

Developing technology platforms to enable robust on site elastic fiber repair would fulfill a major requirement in regenerative therapeutics, and could be critical in treating several proteolytic vascular disorders. Results from this study provide strong evidence that EVs derived from BM-MSCs are a critical and necessary component of the paracrine secretions of cells contained in their conditioned medium, which mediating elastic matrix regenerative and anti-proteolytic effects. Although detailed investigations are required to elucidate the actual mechanism by which EVs exert their regenerative effects, this study opens up a new perspective in developing cell-free surrogate approach for elastic matrix regenerative repair in the AAA wall.

Supplementary Material

Refer to Web version on PubMed Central for supplementary material.

Acknowledgments

References

1. Wills A, Thompson M, Crowther M, Sayers R, Bell P, Pathogenesis of abdominal aortic aneurysms—cellular and biochemical mechanisms, Eur. J. Vasc. Endovasc. Surg. 12 (1996) 391–400. [PubMed: 8980425]

2. Kadoglou NP, Liapis CD, Matrix metalloproteinases: contribution to pathogenesis, diagnosis, surveillance and treatment of abdominal aortic aneurysms, Curr. Med. Res. Opin. 20 (2004) 419–432. [PubMed: 15119978]

3. Crowther M, Goodall S, Jones JL, Bell PR, Thompson MM, Increased matrix metalloproteinase 2 expression in vascular smooth muscle cells cultured from abdominal aortic aneurysms, J. Vasc. Surg. 32(3) (2000) 575–583. [PubMed: 10957667]

4. Mithieux SM, Weiss AS, Elastin, Adv. Protein Chem. 70 (2005) 437–461. [PubMed: 15837523]

5. Kielty CM, Elastic fibres in health and disease, Expert Rev. Mol. Med. 8 (2006) 1–23.

6. Wagenseil JE, Mecham RP, New insights into elastic fiber assembly, Birth Defects Res. C Embryo Today 81(2007) 229–240. [PubMed: 18228265]

7. Bashur CA, Venkataraman L, Ramamurthi A, Tissue engineering and regenerative strategies to replicate biocomplexity of vascular elastic matrix assembly, Tissue Eng. Part B Rev. 18 (2012) 203–217. [PubMed: 22224468]

8. Sivaraman B, Bashur CA, Ramamurthi A, Advances in biomimetic regeneration of elastic matrix structures, Drug Deliv. Transl. Res. 2 (2012) 323–350. [PubMed: 23355960]

9. McMahon MP, Faris B, Wolfe BL, Brown KE, Pratt CA, Toselli P, Franzblau C, Aging effects on the elastin composition in the extracellular matrix of cultured rat aortic smooth muscle cells, In Vitro Cell Dev. Biol. 21 (1985) 674–680. [PubMed: 3908442]

10. Trohatou O, Roubelakis MG, Mesenchymal stem/stromal cells in regenerative medicine: past, present, and future, Cell Reprogram. 19 (2017) 217–224. [PubMed: 28520465]

11. Gurusamy N, Alsayari A, Rajasingh S, Rajasingh J, Adult stem cells for regenerative therapy, Prog. Mol. Biol. Transl. Sci. 160 (2018) 1–22. [PubMed: 30470288]

12. Chamberlain G, Fox J, Ashton B, Middleton J, Concise review: mesenchymal stem cells: their phenotype, differentiation capacity, immunological features, and potential for homing, Stem cells 25 (2007) 2739–2749. [PubMed: 17656645]

13. Ryan JM, Barry FP, Murphy JM, Mahon BP, Mesenchymal stem cells avoid allogeneic rejection, J. Inflamm. (Lond). 2 (2005) 8. [PubMed: 16045800]

14. Swaminathan G, Gadepalli VS, Stoilov I, Mecham RP, Rao RR, Ramamurthi A, Proelastogenic effects of-derived smooth muscle cells on cultured aneurysmal smooth muscle cells, J. Tissue Eng. Regen. Med. 11 (2017) 679–693. [PubMed: 25376929]

15. Swaminathan G, Stoilov I, Broekelmann T, Mecham R, Ramamurthi A, Phenotype-based selection of bone marrow mesenchymal stem cell-derived smooth muscle cells for elastic matrix regenerative repair in abdominal aortic aneurysms, J. Tissue Eng. Regen. Med. 12(2018) e60–e70. [PubMed: 27860330]

16. Ankrum J, Karp JM, Mesenchymal stem cell therapy: Two steps forward, one step back, Trends Mol. Med. 16 (2010) 203–209. [PubMed: 20335067]

17. Mohseny AB, Hogendoorn PC, Concise review: mesenchymal tumors: when stem cells go mad, Stem cells 29 (2011) 397–403. [PubMed: 21425403]

18. Gnecchi M, Zhang Z, Ni A, Dzau VJ, Paracrine mechanisms in adult stem cell signaling and therapy, Circ. Res. 103 (2008) 1204–1219. [PubMed: 19028920]

19. Raposo G, Stoorvogel W, Extracellular vesicles: exosomes, microvesicles, and friends, J. Cell Biol. 200 (2013) 373–383. [PubMed: 23420871]

20. Simons M, Raposo G, Exosomes–vesicular carriers for intercellular communication, Curr. Opin. Cell Biol. 21(2009) 575–581. [PubMed: 19442504]

21. Lötvall J, Hill AF, Hochberg F, Buzás EI, Di Vizio D, Gardiner C, Gho YS, Kurochkin IV, Mathivanan S, Quesenberry P, Minimal experimental requirements for definition of extracellular vesicles and their functions: a position statement from the International Society for Extracellular Vesicles, J. Extracell. Vesicles 3 (2014) 26913.

22. Vlassov AV, Magdaleno S, Setterquist R, Conrad R, Exosomes: current knowledge of their composition, biological functions, and diagnostic and therapeutic potentials, Biochim. Biophys. Acta Gen. Subj. 1820 (2012) 940–948.

23. Théry C, Amigorena S, Raposo G, Clayton A, Isolation and characterization of exosomes from cell culture supernatants and biological fluids, Curr. Protoc. Cell Biol. 30 (2006) 3.22. 1–3.22. 29.

24. Anidjar S, Salzmann J-L, Gentric D, Lagneau P, Camilleri J-P, Michel J-B, Elastase-induced experimental aneurysms in rats, Circulation 82 (1990) 973–981. [PubMed: 2144219]

25. Deb PP, Ramamurthi A, Spatiotemporal mapping of matrix remodelling and evidence of in situ elastogenesis in experimental abdominal aortic aneurysms, J. Tissue Eng. Regen. Med. 11 (2017) 231–245. [PubMed: 24799390]

26. Gacchina CE, Deb P, Barth JL, Ramamurthi A, Elastogenic inductability of smooth muscle cells from a rat model of late stage abdominal aortic aneurysms, Tissue Eng. Part A. 17 (2011) 1699–1711. [PubMed: 21341992]

27. Camardo A, Seshadri D, Broekelmann T, Mecham R, Ramamurthi A, Multifunctional JNK-inhibiting nanotherapeutics for augmented elastic matrix regenerative repair in aortic aneurysms, Drug Deliv. Transl. Res. 8 (2018) 964–984. [PubMed: 28875468]

28. Newman KM, Jean-Claude J, Li H, Ramey WG, Tilson MD, Cytokines that activate proteolysis are increased in abdominal aortic aneurysms, Circulation 90 (1994) II224–7.

29. Dahal S, Broekelman T, Mecham RP, Ramamurthi A, Maintaining elastogenicity of mesenchymal stem cell-derived smooth muscle cells in two-dimensional culture, Tissue Eng. Part A. 24 (2018) 979–989. [PubMed: 29264957]

30. Livak KJ, Schmittgen TD, Analysis of relative gene expression data using real-time quantitative PCR and the 2− CT method, Methods 25 (2001) 402–408. [PubMed: 11846609]

31. Sivaraman B, Swaminathan G, Moore L, Fox J, Seshadri D, Dahal S, Stoilov I, Zborowski M, Mecham R, Ramamurthi A, Magnetically-responsive, multifunctional drug delivery nanoparticles for elastic matrix regenerative repair, Acta Biomater. 52 (2017) 171–186. [PubMed: 27884774]

32. Labarca C, Paigen K, A simple, rapid, and sensitive DNA assay procedure, Anal. Biochem. 102 (1980) 344–352. [PubMed: 6158890]

33. Stoilov I, Starcher BC, Mecham RP, Broekelmann TJ, Measurement of elastin, collagen, and total protein levels in tissues, Methods Cell Biol.143 (2018) 133–146. [PubMed: 29310774]

34. Mecham RP, Broekelmann TJ, Fliszar CJ, Shapiro SD, Welgus HG, Senior RM, Elastin degradation by matrix metalloproteinases Cleavage site specificity and mechanisms of elastolysis, J. Biol. Chem. 272(29) (1997) 18071–18076. [PubMed: 9218437]

35. Mendez MG, Kojima S-I, Goldman RD, Vimentin induces changes in cell shape, motility, and adhesion during the epithelial to mesenchymal transition, FASEB J. 24 (2010) 1838–1851. [PubMed: 20097873]

36. McKelvey KJ, Powell KL, Ashton AW, Morris JM, McCracken SA, Exosomes: mechanisms of uptake, J. Circ. Biomark. 4 (2015) 7. [PubMed: 28936243]

37. Goodall S, Crowther M, Hemingway DM, Bell PR, Thompson MM, Ubiquitous elevation of matrix metalloproteinase-2 expression in the vasculature of patients with abdominal aneurysms, Circulation 104(2001) 304–309. [PubMed: 11457749]

38. McMillan WD, Tamarina NA, Cipollone M, Johnson DA, Parker MA, Pearce WH, Size matters: the relationship between MMP-9 expression and aortic diameter, Circulation 96 (1997) 2228–2232. [PubMed: 9337194]

39. Sivaraman B, Ramamurthi A, Multifunctional nanoparticles for doxycycline delivery towards localized elastic matrix stabilization and regenerative repair, Acta Biomater. 9 (2013) 6511–6525. [PubMed: 23376127]

40. Choudhury R, McGovern A, Ridley C, Cain SA, Baldwin A, Wang M-C, Guo C, Mironov A, Drymoussi Z, Trump D, Differential regulation of elastic fiber formation by fibulin-4 and-5, J. Biol. Chem. 284 (2009) 24553–24567. [PubMed: 19570982]

41. Cobb MH, MAP kinase pathways, Prog biophys mol biol. 71 (1999) 479–500. [PubMed: 10354710]

42. Ghosh A, DiMusto PD, Ehrlichman LK, Sadiq O, McEvoy B, Futchko JS, Henke PK, Eliason JL, Upchurch GR Jr, The role of extracellular signal-related kinase during abdominal aortic aneurysm formation, J. Am. Coll. Surg. 215 (2012) 668–680. [PubMed: 22917644]

43. Wang Y, Krishna S, Walker PJ, Norman P, Golledge J, Transforming growth factor-β and abdominal aortic aneurysms, Cardiovasc. Pathol. 22 (2013) 126–132. [PubMed: 22959236]

44. Doyle JJ, Gerber EE, Dietz HC, Matrix-dependent perturbation of TGFβ signaling and disease, FEBS Lett. 586 (2012) 2003–2015. [PubMed: 22641039]

45. Shelke GV, Yin Y, Jang SC, Lässer C, Wennmalm S, Hoffmann HJ, Li L, Gho YS, Nilsson JA, Lötvall J, Endosomal signalling via exosome surface TGFβ–1, J. Extracell. Vesicles 8 (2019) 1650458.

46. Wang M, Zhao D, Spinetti G, Zhang J, Jiang L-Q, Pintus G, Monticone R, Lakatta EG, Matrix metalloproteinase 2 activation of transforming growth factor-β1 (TGF-β1) and TGF-β1–type II receptor signaling within the aged arterial wall, Arterioscler. Thromb. Vasc. Biol. 26 (2006) 1503–1509.

47. Gacchina C, Brothers T, Ramamurthi A, Evaluating smooth muscle cells from CaCl2-induced rat aortal expansions as a surrogate culture model for study of elastogenic induction of human aneurysmal cells, Tissue Eng. Part A 17 (2011) 1945–1958. [PubMed: 21417692]

Statement of Significance

Abdominal aortic aneurysms (AAAs) are localized, rupture-prone expansions of the aorta which result from loss of wall flexibility due to enzymatic breakdown of elastic fibers. There are no established alternatives to surgery, which possess high risk for the mostly elderly patients. Our previous studies have established the elastic regenerative and reparative effect of cell culture secretions derived from adult stem cell source. In this study, we propose to isolate extracellular vesicles (exosomes) from these secretions and evaluate their regenerative benefits in AAA smooth muscle cell culture model. This simple and innovative treatment approach has the potential to arrest or reverse AAA growth to rupture, not possible so far.
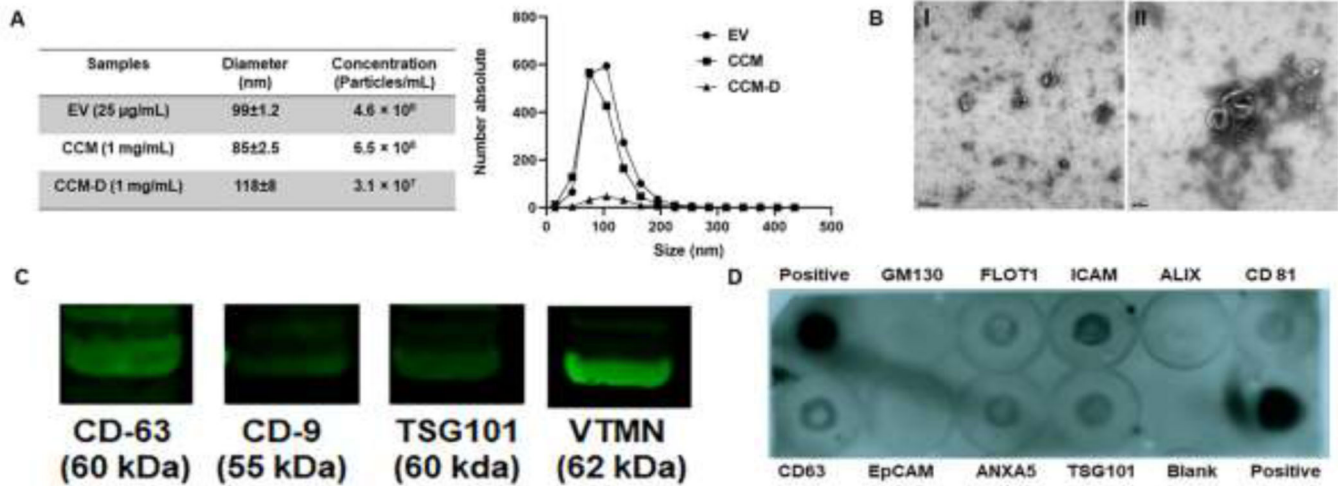
Figure 1. Characterization of EVs.

(A) Nanoparticle tracking analysis (NTA) of EV, CCM and CCM-D samples. EV samples contained 25 μg/ml of total protein, CCM and CCM-D samples were used at a protein concentration of 1 mg/mL. Average size and particle content in each samples are provided in the table. (B) TEM images of EVs. Scale bar = 200 nm (I), 100 nm (II). (C) Western Blot (WB) analysis of common EV marker proteins (CD-63, CD-9, TSG 101 and Vimentin) detected using their mouse monoclonal antibodies. (D) Common exosomal markers identified using an Exo-Check™ Exosome Antibody Array. Blank spot serves as background control and GM130 control shows levels of cellular contamination in EV preparations. Protein ID and descriptions are provided in the tabular format in the supplementary Table S1.
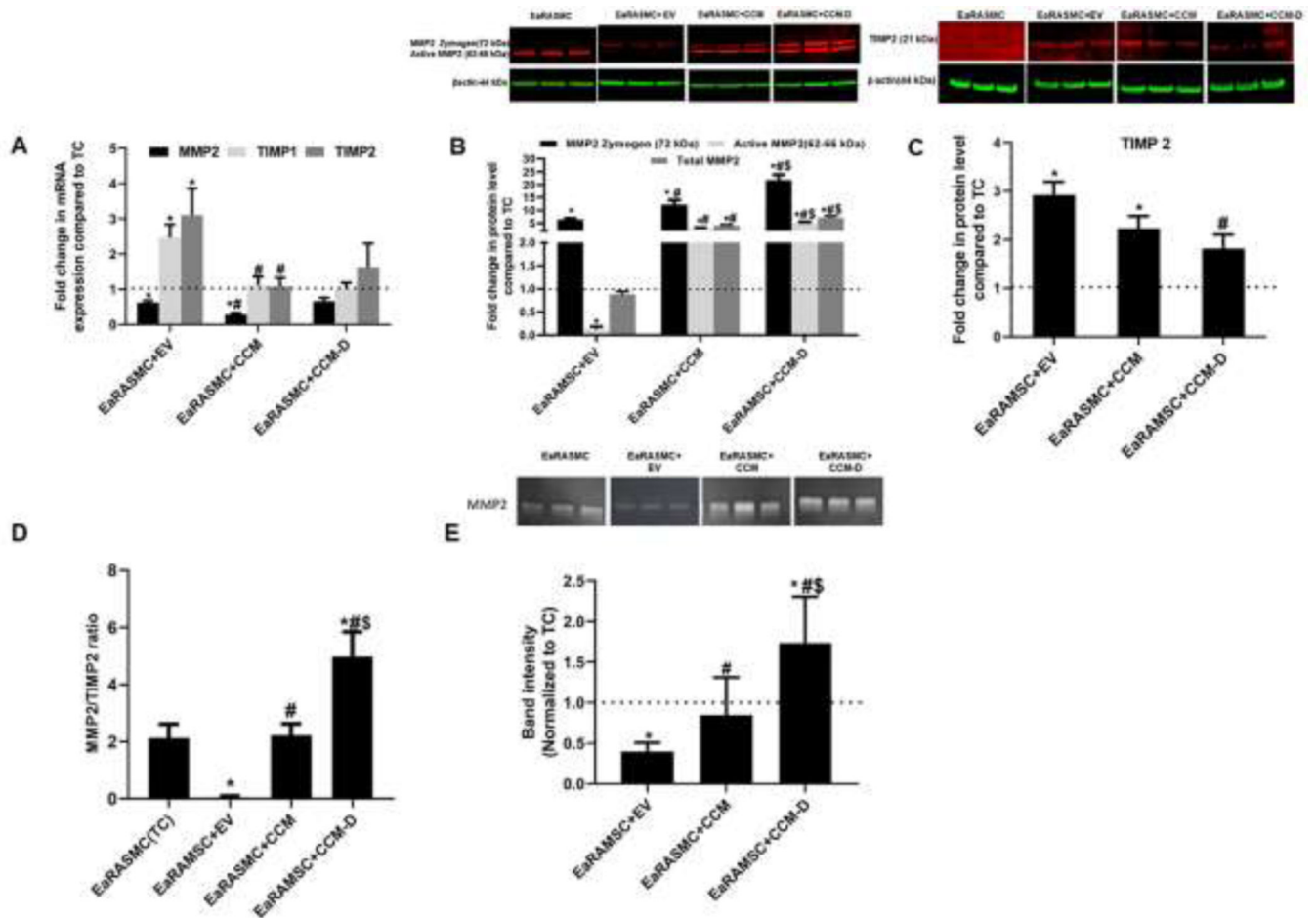
Figure 2. Effect of EV/CCM/CCM-D treatment on anti-proteolytic signaling proteins (MMP2 and TIMP2) expression in an EaRASMC culture model.
(A) Relative gene expression of MMP2/TIMP1/TIMP2 analyzed by RT-PCR. (B, C) WB analysis of β-actin normalized expression of MMP 2 and TIMP 2 proteins shown relative to values in treatment control cultures (TC). (D) Ratio of intensities of active MMP2 and TIMP2 bands on WB. (E) Gel zymogram analysis for MMP-2 enzymatic activity. In all plots, values shown indicate mean ± SE of measurements made in n = 6 replicate cultures per condition. * denotes $p < 0.05$ compared to TC cultures, # denotes $p < 0.05$ compared to EV treated samples, $ denotes $p < 0.05$ compared to CCM treated sample.
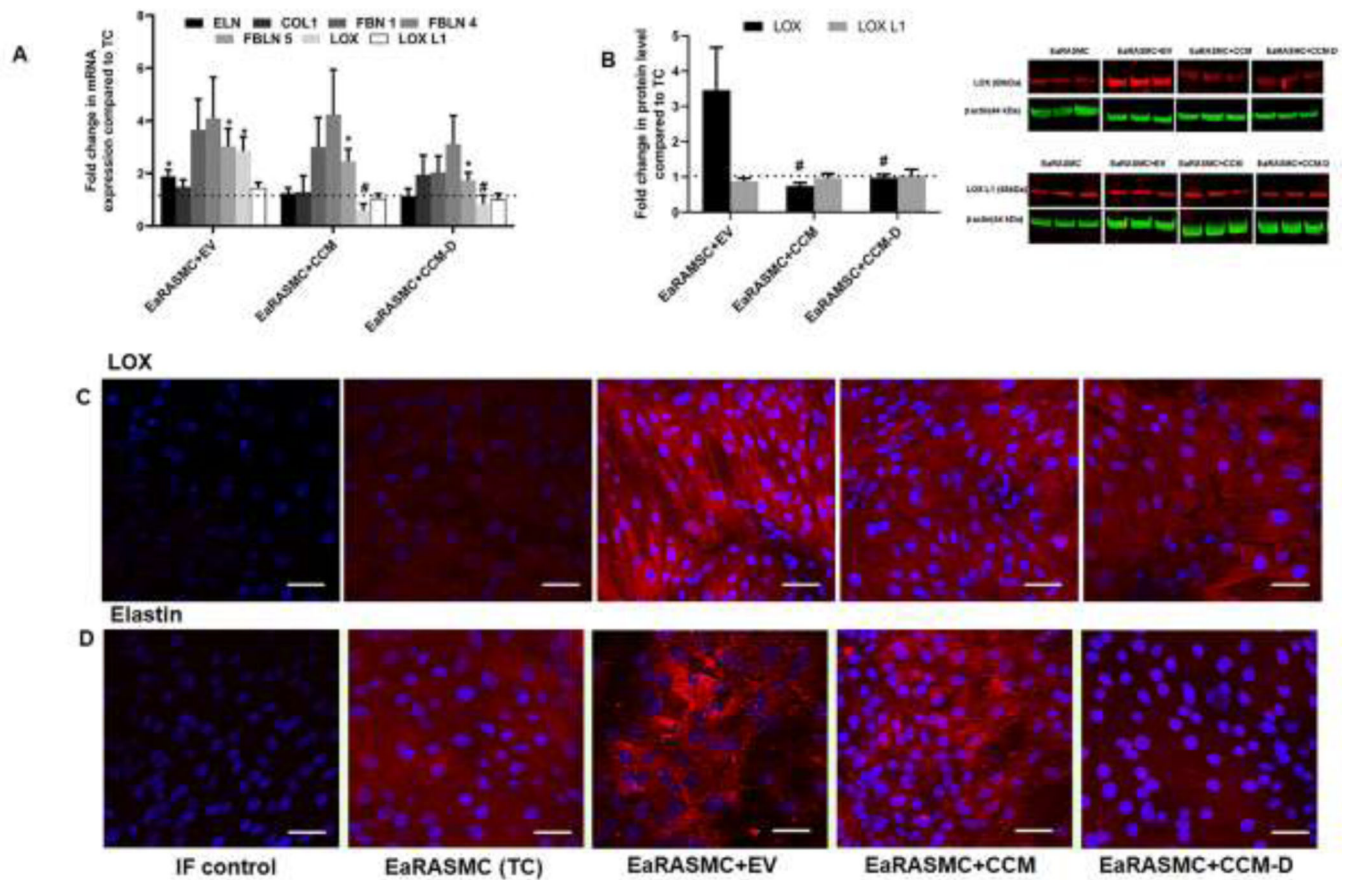
Figure 3. Effects of EV/CCM/CCM-D treatment on the expression of key elastic fiber assembly proteins in an EaRASMC culture model.

(A) Relative gene expression of key proteins involved in elastic fiber assembly and homeostasis analyzed by RT-PCR. (B) WB analysis for expression of elastin crosslinking proteins LOX and LOXL1. Protein band intensities were normalized to respective β-actin bands and values were then further normalized to the ratios obtained in treatment control (TC) cultures. In all plots, values shown indicate mean ± SE of measurements made in n = 6 replicated cultures per condition. *denotes p < 0.05 compared to TC cultures, # denotes p < 0.05 compared to EV treated samples, $ denotes p < 0.05 compared to CCM treated sample. Immunofluorescence (IF) micrographs showing expression of LOX (C), and elastin (D) deposition in EaRASMC cultures Cells nuclei were stained with DAPI (blue) and the proteins of interest visualized with a secondary antibody conjugated to an Alexa Fluor 568 dye (red). Scale bars in C and D: 50μm.
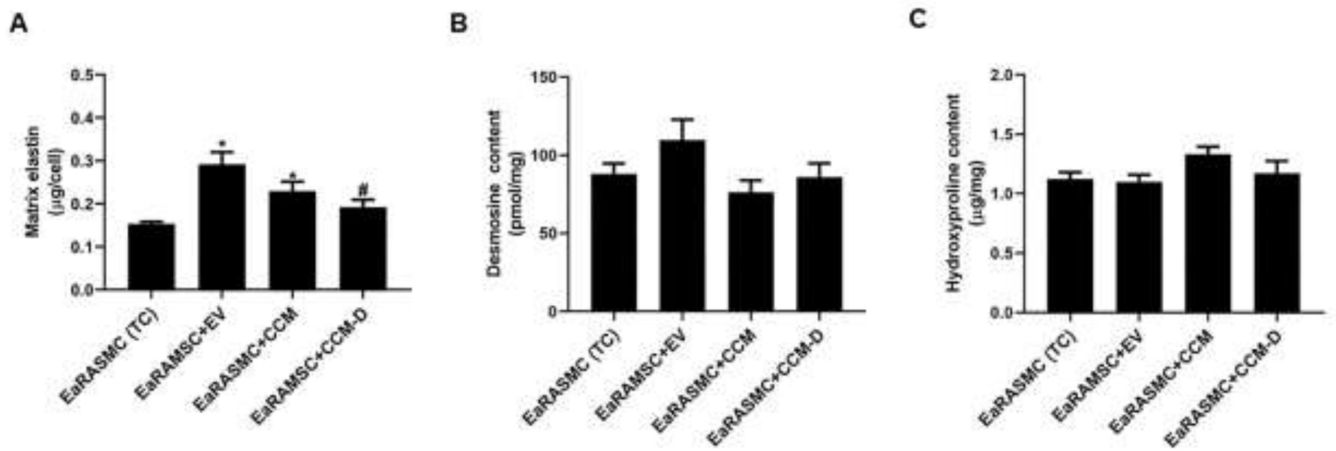
Figure 4. Effects of EV/CCM/CCM-D treatment on elastic matrix deposition and crosslinking in EaRASMC cultures.

(A) Total matrix elastin amounts in culture groups measured using a Fastin assay, shown normalized to cell content in the respective cultures. (B) Desmosine (elastin crosslinker) content in cultures shown normalized to total protein amounts in the respective cultures. (C) Matrix collagen content estimated by hydroxyproline (OH-Pro) assay. Values shown in plots indicate mean ± SE of measurements made in n = 6 replicate cultures per condition. * denotes p < 0.05 compared to TC cultures, # denotes p < 0.05 compared to EV treated samples, $ denotes p < 0.05 compared to CCM treated sample.
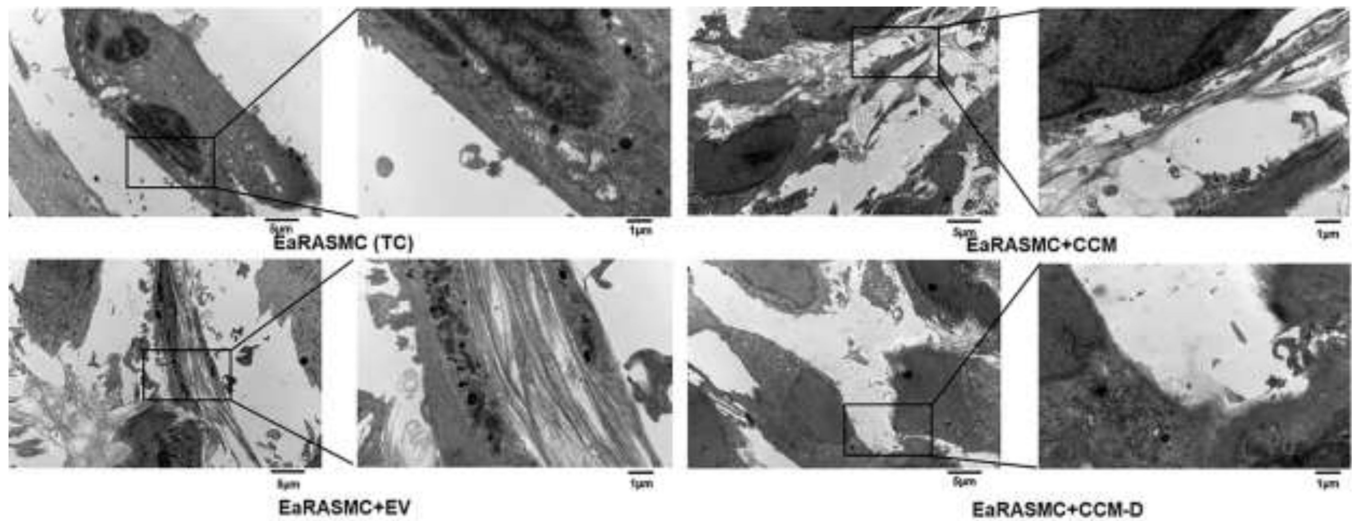
Figure 5. Effects of EV/CCM/CCM-D treatment on elastic fiber ultrastructure.
Transmission electron micrographs showing elastic fiber formation (red arrows) in EaRASMC cultures treated with EVs/CCM/CCM-D. TC and CCM-D treated cell layers contained very few sporadic deposits of elastin and no fibers. In all cases, the cells were cultured for 21 days and treated with either EVs (25 μg/ml; total protein concentration) or CCM/CCM-D (1 mg/mL; total protein concentration) samples for a period of 24 h on a weekly basis.
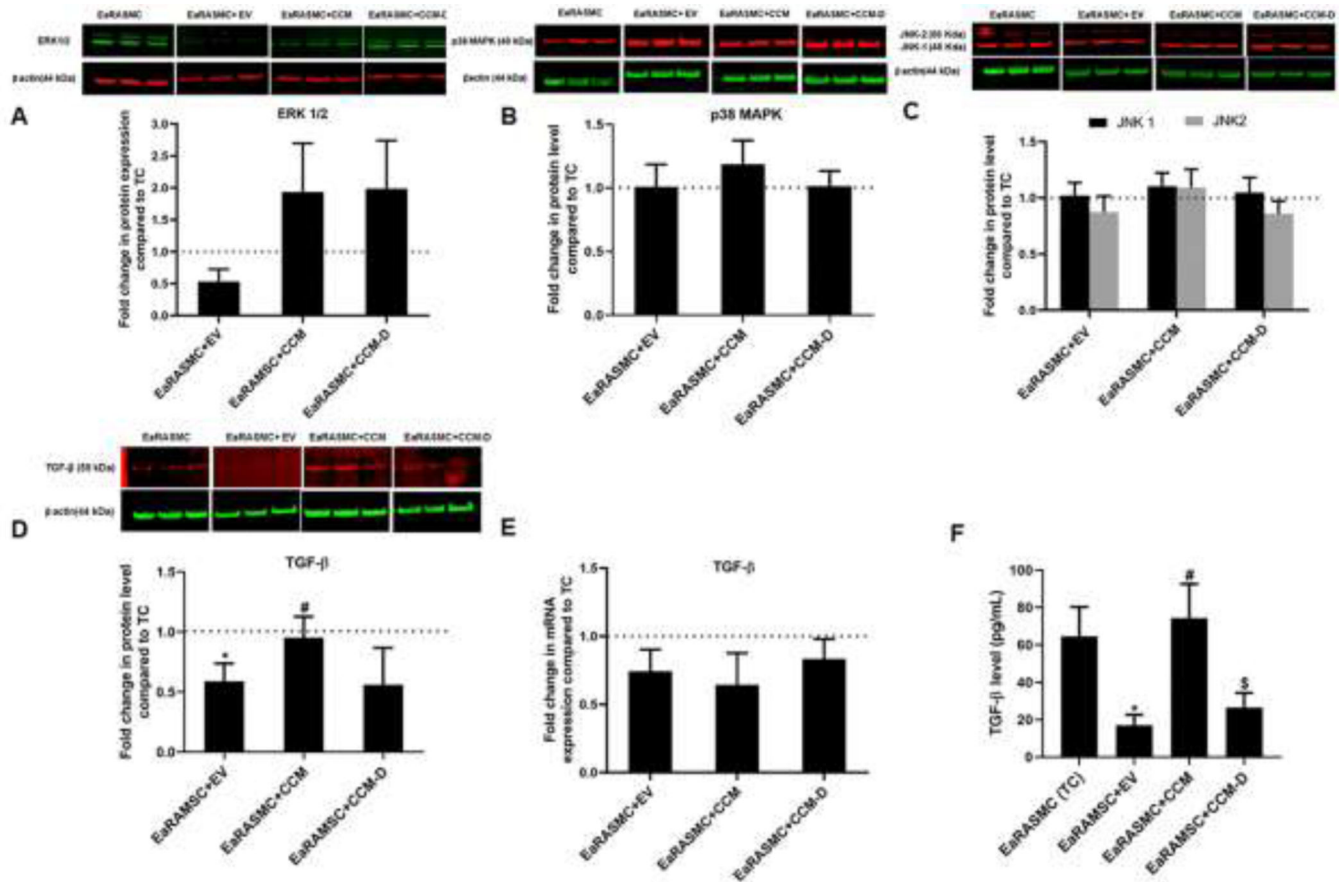
Figure 6. Effects of EV/CCM/CCM-D treatment on expression of key signaling proteins known to regulate ECM homeostasis in proteolytic disorders.

Shown are WB analysis results indicating effects of treatment on protein expression of ERK1/2 (A), p38MAPK (B), JNK1/2 (C) and TGF-β1 (D). Panel E shows effect of treatment on gene expression of TGF-β1 as analyzed using RT-PCR and panel F shows levels of mature TGF-β1 secreted into culture medium measured using a sandwich ELISA method. In all plots, values shown indicate mean ± SE of measurements made in n = 6 replicate cultures per condition. * denotes $p < 0.05$ compared to TC cultures, # denotes $p < 0.05$ compared to EV treated samples, $ denotes $p < 0.05$ compared to CCM-treated cultures.
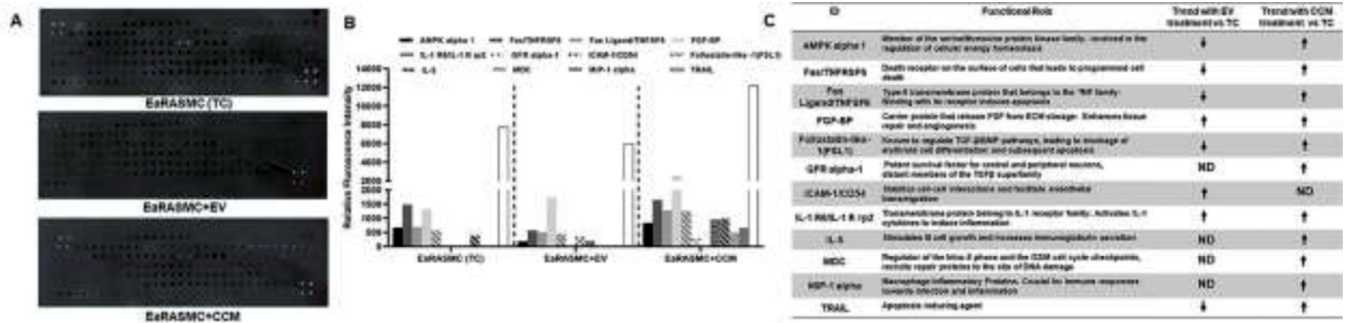
Figure 7. Effects of EV and CCM treatment on cytokine expression in EaRASMC cultures.
Rat L 90 Antibody Array based evaluation on relative cytokine expression on EaRASMC culture, following treatment with EV or CCM. (A) Scanning images of array obtained using GenePix laser scanner. (B) Semi-quantitative analysis of blots based on relative florescence intensity obtained using GenePix Pro® software. Cell layers for L90 analysis were cultured for 14 days and treated with either EVs (25 μg/ml; total protein concentration) or CCM (1 mg/mL; total protein concentration) for a period of 24 h. Protein ID and descriptions are provided in the Table in panel C.

Table 1.

List of primers used in the study

Gene	Forward primer (5′→3′)	Reverse primer (5′→3′)
18s	CGGACAGGATTGACAGATTG	ACGCCACTTGTCCCTCTAAG
MMP2	CTGCCCAGAGACTGCTATGT	TTCCGGTCATCATCGTAGTT
MMP9	ACTTCTGGCGTGTGAGTTTC	TGTATCCGGCAAACTAGCTC
TIMP1	CATGGAGAGCCTCTGTGGAT	ATGGCTGAACAGGGAAACAC
TIMP2	CTCCGAGTGCTGTTACGATT	TCCATGCTGTGGTAATGTTG
TGF-β1	CGGACTACTACGCCAAAGAA	TTGCTCCACAGTTGACTTGA
ELN	TAGCTCCCTTGTTCTTGTGG	CCGCCTTAGCAGCAGATTTGG
COLA1	GTACTGCATGTGGGAAGGGAC	AGCACCATCATTTCCACGA
LOX	AGACGATTTGCCTGTACTGC	ATAGGCGTGATGTCCTGTGT
LOX L1	CTCCGAGTGCTGTTACGATT	TCCATGCTGTGGTAATGTTG
FBN1	ATAAATGAATGTGCCCAGAATCCC	ACTCATCCTCATCTTTACACATCC
FBLN4	CACGGAATGCACAGATGGCTA	TGTCCACACAGCTCTCCTGTT
FBLN 5	AGGGACAGGAGGAGAGAAGA	AAGGCCTTGGAGAGTCACTT